

## Active Handrest for Precision Manipulation and Ergonomic Support

Mark A. Fehlberg, Brian T. Gleeson, Levi C. Leishman, and William R. Provancher  
Haptics and Embedded Mechatronics Lab, University of Utah

### ABSTRACT

People use handrests every day to complete dexterous activities as routine as providing a signature. However, the dexterous workspace of the hand is somewhat limited. To address this limit, we have developed an Active Handrest to aid in precision manipulation tasks by extending a user's dexterous work space while providing ergonomic support for reduced fatigue – ideally while maintaining or even improving upon the precision obtained from a fixed handrest. Such a device could be useful for performing precision tasks over large workspaces, such as surgery, machining, or pick-and-place tasks. Our current prototype Active Handrest is a planar, computer controlled support for the user's wrist and arm that allows the user complete control over a grasped tool or manipulation device. The device uses force input from the user's hand, position input from a grasped manipulandum, or a combination of both force and position inputs. The control algorithm of the device then interprets and converts the input(s) into handrest motions. Pilot studies were conducted to optimize the control strategy by investigating the effects of control mode and of velocity limits. Task precision and completion time were used as performance metrics. Pilot testing showed that the device provided the greatest task precision when its velocity was limited to 5 mm/s, while using force input for its control strategy. An experiment was then conducted to compare the Active Handrest to various fixed wrist and arm support conditions, as well as the unsupported condition. Use of the Active Handrest was found to reduce task error by 36.6%, compared to performing the tasks with an unsupported arm, and by 26.0% compared to task completion with a static wrist support. These results are statistically significant ( $p < 0.0001$ ). While users generally completed experiments more slowly using the Active Handrest, performance with the Active Handrest shows lower sensitivity of task error relative to task completion time. Added experience with our drawing task leads to an increase in accuracy; however, the Active Handrest continues to outperform other hand support conditions ( $p < 0.0001$ ).

**KEYWORDS:** precision manipulation, fatigue reduction, haptic device design, handrest, velocity limits

**INDEX TERMS:** human factors and ergonomics, dynamic systems and control, assistive technology, haptic perception and psychophysics

### 1 INTRODUCTION

Handrests have been used in many applications to improve precision and reduce fatigue. Traditionally, handrests are static, providing support in only a small workspace. For example, the

---

Department of Mechanical Engineering  
50 S. Central Campus Drive, Salt Lake City, UT, 84112-9208  
m.fehlberg@utah.edu, {brian.gleeson, levileishman}@gmail.com,  
wil@mech.utah.edu

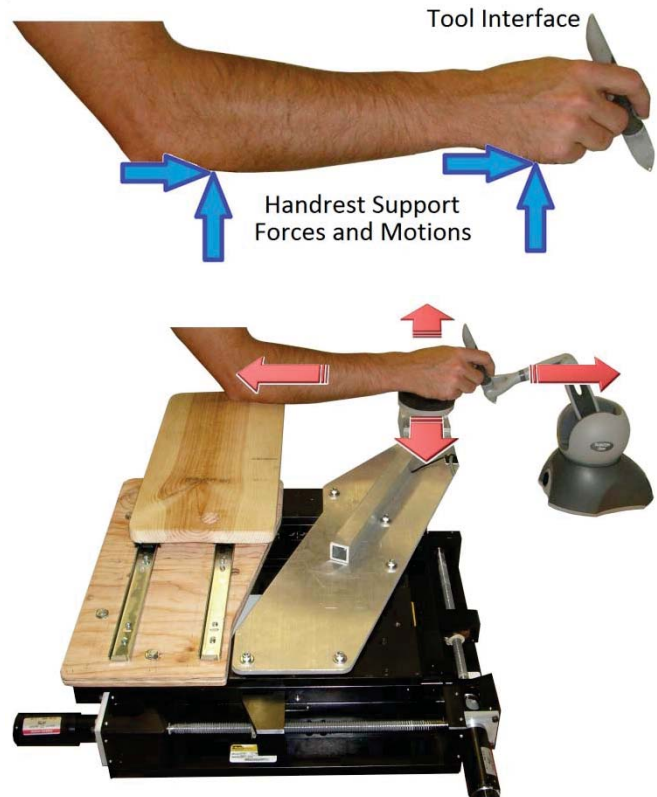


Figure 1. Active Handrest concept (top) and prototype (bottom).

hand's dexterous workspace may be as large as 10 cm when sketching using a fixed wrist position, or as small as 2-3 cm when painting fine details such as facial features in a portrait. Repositionable handrests allow for multiple small workspaces and requires time for repositioning, rather than directly increasing a user's dexterous workspace. A mobile handrest could aid in obtaining high precision and improved support over a workspace with size several orders of magnitude larger than obtained using a static handrest. In this paper, we present the development of the Active Handrest, a device that steadies the user's hand while allowing for continuous repositioning throughout a task area (Fig. 1). The purpose of this device is to provide a local basis of support for the user to perform precision manipulation. The Active Handrest is designed to continuously reposition itself such that the user's hand remains near the center of its dexterous workspace. The challenge is to do this repositioning task in a manner that does not result in a loss of precision, such as would be predicted by Fitts' Law. The Active Handrest could be useful for assisting a user in performing a variety of precision tasks with reduced fatigue over a large workspace. The Active Handrest would benefit surgeons and other medical personnel [1, 2], artists, machinists, workers performing pick-and-place tasks, or anyone requiring dexterous control of tools. In this paper we present background on various haptic device control strategies and also

examine limiting the velocity and acceleration of our device to improve task accuracy. We then describe our device and an experiment which evaluates the performance of the Active Handrest versus other hand support conditions. Results of this experiment are discussed, along with suggested future work.

## 2 BACKGROUND

There are several possible means of providing ergonomic support for a person's hand while he or she performs dexterous tasks. For example, people often brace their wrist or arm against a fixed object to increase precision. Static rests are often used while typing or while using a computer mouse. There are also many different methods of repositionable hand supports that have been explored. Artists often use repositionable braces to rest and steady the brush hand while painting fine details on a large canvas. Other devices allow for repositionable support while typing. In addition to providing increased precision, hand and arm rests have been shown to reduce user muscle fatigue [3].

More recent research has focused on robots assisting a user in manipulating a tool. For example, devices such as Steady Hand, which allows the tool to be simultaneously held by both the user and a robot, aid a user in performing precision tasks [4]. Other cooperative human/robot devices such as Cobots passively constrain a user's motion [5]. Virtual fixtures have often been employed to guide a user on an intended path or prevent a user from operating in a forbidden zone [1, 6-8]. In all of these devices, control of the tool is shared between the human and the robot. In contrast, the Active Handrest provides ergonomic support and increased precision, but allows the user to maintain complete control of the tool. Furthermore, the Active Handrest can be used with any tool, and the tool need not be the end-effector of a robotic linkage.

To ensure that the Active Handrest was optimized for precision manipulation, we considered several factors in our controller. The first factor considered was the input mode from the user. We also gave consideration to whether limiting the device's velocity and acceleration would increase a user's precision.

In examining the input mode from the user to our device, we designed the controller to accept desired velocity and position data from either isotonic/position input, isometric/force input, or a blend of force and position inputs. Previous work has shown that while isotonic controllers lead to shorter task completion times, their movements are less precise than isometric controllers [9]. Other work has shown that elastic (blend of isometric and isotonic) rate control initially increases task completion times over isometric controllers, but that learning eventually equalizes completion times regardless of the control strategy used [10].

The second factor examined was the effect of limiting the Active Handrest's velocity and acceleration. In [11] it was shown that velocity limits determine force control precision. In an attempt to eliminate any difficulties in maintaining force control precision during start up and termination of individual device movements, as observed in [11], we added acceleration limiting to our controller. Velocity and acceleration limits were applied under position (isotonic), force (isometric), and blended (mixture of isotonic and isometric) control.

## 3 DEVICE DESCRIPTION

The motion of the Active Handrest (Fig. 2) is provided by a Parker two-axis linear stage. Sensed force input is provided by an interaction between the user's hand and a round pad. Sensed position input is provided by the user's manipulation of a grasped Phantom Omni stylus. Force and position input data are collected by a Sensoray 626 data acquisition card at 1 kHz. The input data are then processed by our controller on a PC running C++ code with CHAI-3D libraries operating in a Windows 7 environment.

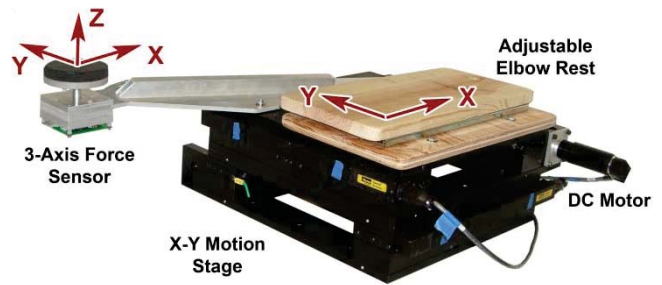


Figure 2. This Active Handrest prototype consists of a Parker two-axis linear stage driven by geared DC motors, and includes an elbow rest and instrumented handrest at the end of a cantilevered support arm.

The controller outputs motor commands through the Sensoray card which are amplified before being sent to the stage's motors.

While interacting with the Active Handrest, the user's right hand and/or wrist are rested on the round, force sensing pad at the end of a support arm attached to the stage. The force sensing pad is fixed relative to the motion axes and allows no rotation. The user's right elbow rests on an adjustable elbow rest attached to the back side of the stage, shown in Fig. 2. The user grasps the Omni stylus with his or her right hand. The stylus provides input for our experiment's drawing task and position input to the Active Handrest's controller.

The Parker stage is driven by two 4.8:1 geared Maxon RE36 DC motors. Position is measured by 500 cpr optical encoders operating in quadrature. This drive-train provides a position resolution of approximately 0.26  $\mu\text{m}$ ; however after accounting for backlash, positioning resolution is estimated at 5  $\mu\text{m}$ . The stage has a workspace of 26.6 cm x 26.6 cm between its hard stops. Hardware limit switches in this prototype design were conservatively installed approximately 3 cm from the hard stops, and software limits further reduced the current workspace. Conservative limits on the stage's motion were implemented to protect the device in part due to the uncertainty of the user's interaction with the Active Handrest. These limits were also implemented to better match the workspace of the Omni stylus, which at the height of the drawing plane was approximately 12 x 16 cm. Despite these limits, results from these experiments extend to arbitrarily large workspaces.

There are two available controller inputs: force from the custom force sensor and position from the Omni. Each of these inputs is able to control the Active Handrest independently or they can be blended to implement hybrid control of the device by weighting the two inputs.

The contact force between the user's hand and the device is measured using a three-axis custom force sensor (Fig. 3), using a Sensoray 626 data acquisition card sampling at 1 kHz. The design and implementation of a custom force sensor was desirable for use in this prototype due to uncertainties in the range of forces that users would impart on the device and a large overload requirement for the force sensor, which also serves as a support for the user's hand. Our custom design allowed for relatively high force sensitivity, while limiting overload forces through mechanical travel stops that capped the forces experienced by the sensing elements. Typical interaction forces during experiments was on order of 1-5 N, while overload forces exceeded 50 N. Use of a commercial force sensor, with a typical overload range  $\sim 2\times$  the operating range, would have resulted in a significant loss of sensitivity in comparison to our custom design.

The force sensor was calibrated to a range of  $\pm 14$  N with a sensitivity of  $\sim 0.8$  mN/bit. The travel of the force sensor was

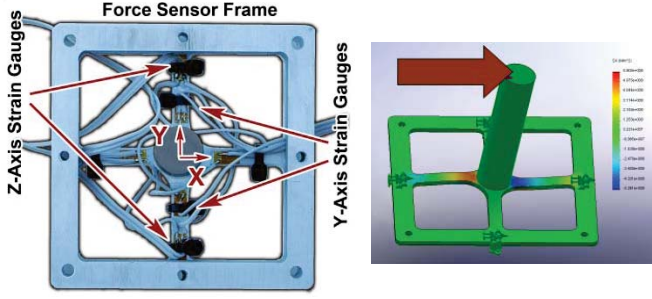


Figure 3. Custom force sensor (left) and force sensor strain analysis (right). Strain gauges are placed in locations of peak strain.

limited with a radial travel stop to avoid inadvertent damage to the sensor's strain gauges. Although this version of the Active Handrest only uses two axes of motion (x and y), the force sensor is designed measure force on all three axes. A z-axis travel stop will also be implemented in the future to prevent damage to the sensor when bearing a user's weight.

The force sensor is comprised of a cross-shaped flexure clamped between two aluminum plates. The flexure is patterned as a 6.35 mm wide cross, made from 1.5 mm thick aluminum. The center of the force sensor has a 51 mm long, 12.7 mm diameter post bolted to it by which forces from the user's hand are coupled into the flexure. The device's handrest is mounted on top of the post. The handrest is a 75 mm diameter, 9.5 mm thick aluminum disk that is covered with 15 mm of foam padding for comfort. The foam padding also allows forces from the user's hand to be transmitted to the force sensor while limiting sliding. The entire force sensor and handrest assembly are bolted to the x-y stage by an aluminum support bracket.

Pairs of strain gauges (Vishay EA-13 120LZ) are bonded to the force sensor's flexure plate to strategically isolate three axes of applied force and maximize linearity on three separate strain bridges. The x (and y) axis is instrumented with a single pair of gauges in radially opposite locations on the flexure plate to form an active  $\frac{1}{2}$ -bridge, as shown in Fig. 3. The finite element analysis (Fig. 3 right) was used to determine that the x-axis gauges should be placed near the center post as this was the location with the highest strain measured in the flexure under laterally applied forces. The z-axis (piercing) is instrumented with a full bridge to increase sensitivity and linearity, as lower strains are induced from z-axis forces. The z-axis gauges were placed on the top and bottom of the flexure at its distal ends (Fig. 3 left). A 5 V linear power supply provides the input for each Wheatstone bridge. The signal from each bridge is amplified using an AD623 instrumentation amplifier before being sent to the Sensoray 626 data acquisition card.

The force sensor was calibrated by applying known loads to each of the three axes. These loads were applied to the center of the Handrest's support pad. Each axis of the sensor was calibrated using ten known masses between 200 g and 2000 g. The force sensor's calibration matrix was calculated using Matlab to compute the right-pseudo inverse of the measurement (voltage) array:

$$\begin{bmatrix} F_x \\ F_y \\ F_z \end{bmatrix} = C * \begin{bmatrix} V_x \\ V_y \\ V_z \end{bmatrix} \Rightarrow C = \begin{bmatrix} F_x \\ F_y \\ F_z \end{bmatrix} * \begin{bmatrix} V_x \\ V_y \\ V_z \end{bmatrix}^{-1} \Rightarrow C = \begin{bmatrix} 8.72 & -0.19 & 0.01 \\ 0.13 & 10.07 & -0.01 \\ -0.50 & 1.36 & 16.56 \end{bmatrix} \quad (1)$$

As can be seen by the low magnitude of the off-diagonal terms, there is very little sensor cross-talk between the axes of the sensor.

The X and Y axes have approximately the same sensitivity (8.72 and 10.07 N/V), while the Z axis is approximately  $\frac{1}{2}$  as sensitive at 16.56 N/V. The linearity of the sensor is approximately 14 mV (120 mN) for the X-axis, 22 mV (220 mN) for the Y-axis, and 20 mV (330 mN) for the Z axis. Variations in sensitivity and linearity between the X and Y axes is likely due to subtle location differences in the installation of the strain gauges on these axes, while larger amplification of the Z-axis strains was responsible for its larger non-linearity. The non-linearity in the X and Y axes, primarily due to hysteresis, was mitigated by implementing a deadband for force sensor inputs.

Relative position information between the manipulandum and the Active Handrest's position is measured using a SensAble Technologies Phantom Omni. Input from the Omni is processed using Phantom drivers ver. 4.2 and OpenHaptics Academic Edition ver. 3.0. The Omni is able to determine position input accurately within 0.055 mm.

The Active Handrest is controlled by a PC running C++ while using Chai3D 2.0.0 libraries in a Windows 7 environment. Position, velocity, and acceleration of the Parker stage are controlled by a 1 kHz servo rate proportional controller with several non-linear modifications implemented to address specific performance issues.

#### 4 DEVICE CONTROL

The overall purpose of the Active Handrest is to provide a local basis of support allowing the user to perform precision manipulation. For example, every time the user's fingertips move from the center of their dexterous workspace, we desire our device to move so that it repositions the user's fingertips back into the center of their dexterous workspace.

Therefore, the goal of the Active Handrest's controller (Fig. 4) is to constantly reposition the device's workspace center to follow the user's dexterous hand-space. To accomplish this task it is necessary for our controller to interpret the user's intent and provide support in that location. The controller interprets user intent by taking inputs of stylus position relative to the stage's position or by interpreting force interaction between the user's hand and the custom force sensor embedded in the handrest's support pad.

The motion of the Active Handrest's stage is controlled by a low-level proportional controller on velocity, which takes desired velocity as an input. The average error in velocity of the proportional controller was found to be less than 5% of the desired velocity. The desired velocity is determined from an admittance controller with specific modifications to accommodate our blended inputs. Overall, the desired handrest velocity is determined by the inputs from the custom force sensor and stylus position. Therefore, the desired velocity  $V$  is equal to an admittance gain  $K_a$  multiplied by the combined force input  $F^*$ .

$$\vec{V} = K_a \vec{F}^* \quad (2)$$

The combined force input is the sum of the force input from the handrest's custom force sensor  $F_{HR}^*$  added to the computed virtual force  $F_{\Delta X}^*$  from the position input.

$$\vec{F}^* = (p) \vec{F}_{\Delta X}^* + (1-p) \vec{F}_{HR}^* \quad (3)$$

The hybrid admittance controller allows us to set the proportion  $p$  of position and force control inputs. The calculated force from the position input is equal to a virtual "spring constant"  $K_s$  multiplied by the difference between the Omni stylus's position and the stage's position.

$$\vec{F}_{\Delta X}^* = K_s (\Delta \vec{x}^*) = K_s (\vec{x}_{STY} - \vec{x}_{STG}) \quad (4)$$

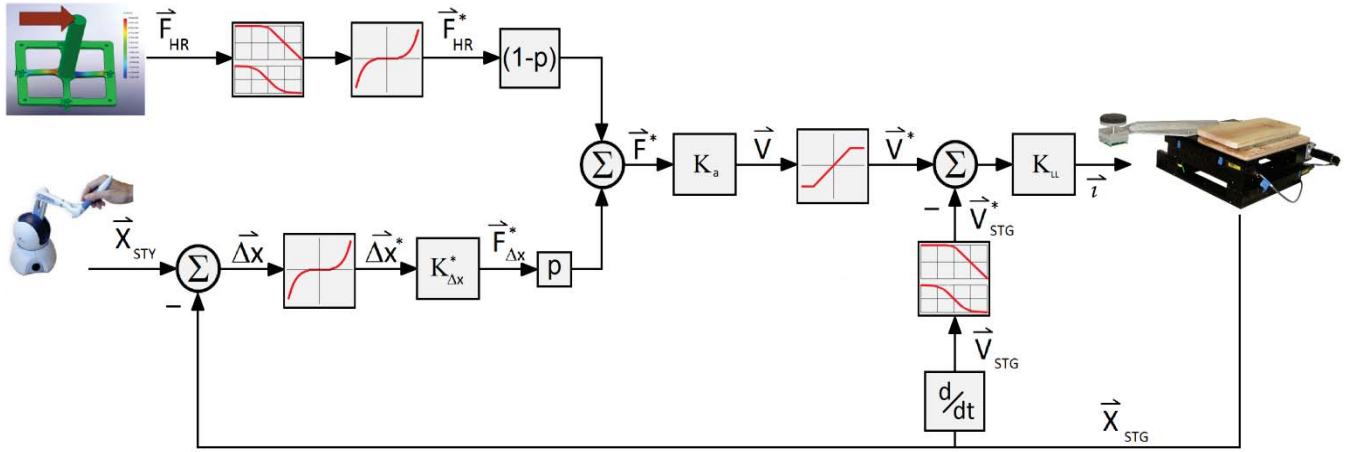


Figure 4. Active Handrest control architecture showing closed loop proportional control of velocity with hybrid admittance controller taking force and position inputs

The actual force from the handrest  $F_{HR}$  is first processed by a low-pass filter with corner frequency of 1.6 Hz. It is then subject to a deadband before being squared to become the term  $F_{HR}^*$ . The force required to exceed the deadband was 200 mN, which was sized relative to the linearity of our force sensor. Likewise, the actual position difference between the stylus and the stage  $F_{\Delta x}$  is also subject to a deadband before being squared to become the term  $\Delta x^*$ . The inputs are squared to allow for a smoother transition from the deadband than a linear relationship would allow and is shown in the 2<sup>nd</sup> filter block on the force input in Fig. 4. Alternatives to squaring the inputs to achieve a smooth transition from the deadband will be investigated in future modifications of the controller.

Before outputting the desired handrest velocity, the signal is processed through acceleration and velocity limiting control blocks. The controller's ability to limit the velocity at which the stage is able to move is implemented as a saturation limit. The saturation is accomplished by setting the desired handrest velocity to the maximum allowed velocity whenever the calculated desired velocity exceeds the maximum allowed velocity. The acceleration limit is implemented by preventing the velocity changes from exceeding the maximum allowed change in velocity for each time step. This process dramatically smoothes the motion of the handrest and allows higher gains to be used without the system becoming unstable.

Completing the explanation of the control diagram in Fig. 4, the current stage velocity is subtracted from the desired velocity to calculate the commanded handrest velocity. The commanded velocity is next multiplied by the low level gain  $K_{LL}$  to convert the commanded velocity to a voltage-to-current signal which is output from the Sensoray 626 data acquisition card.

$$\tilde{i} = K_{LL}(\overline{V_{CMD}}) = K_{LL}(\overline{V^*} - \overline{V_{STG}^*}) \quad (5)$$

The current signal is passed to two linear current amplifiers before being sent to the x-y stage's motors.

## 5 EXPERIMENT: UTILITY OF THE ACTIVE HANDREST

Before beginning the experiment, we first attempted to better tune the control strategy of the Active Handrest by conducting pilot studies to examine the effects of control input, velocity limits, and acceleration limits. It was found that an acceleration limit of 0.5 m/s<sup>2</sup> and a velocity limit of 5 mm/s allowed the greatest accuracy for the Active Handrest regardless of the control input used.

After the control of the Active Handrest had been better understood to provide more optimal interaction, an experiment was conducted to test the utility of the device. The Active Handrest was compared to three fixed hand support conditions (including unsupported).

### 5.1 Methods

All experiments were performed using a circle tracing task. Circle tracing was chosen for simplicity, the unambiguous means for calculating task error (e.g. compared to [12]), and due to the ability to scale uniformly from small, localized tasks to larger, distributed tasks.

While using the Active Handrest, subjects sat with their right arm in contact with both the hand/wrist support pad and the device's elbow rest (Fig. 5 on left). During the experiment a circle was displayed on a computer monitor and subjects used the Omni stylus to trace the circle (Fig. 5 on right). Tracing error and completion time were recorded for each circle. Data points in the drawing task were logged at 100 Hz. These data were used to calculate the tracing error based on a radial projection onto the displayed circle in each trial. Circles were presented, one at a time, at random locations within the device's workspace. After each circle was completed, the user would press the space bar to clear the screen and display the next circle to be drawn. Subjects were asked complete each circle as accurately as possible within a reasonable amount of time. Headphones played white noise to mask any sound from the device and to aid in eliminating distractions.

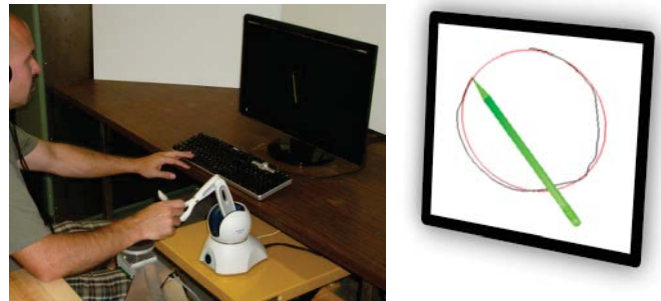


Figure 5. Experiment setup (left) and graphical user interface (right) used for prompting and recording user responses.

Three circle radii were chosen to test a range of precisions tasks. A 7.5 mm radius circle tested high curvature drawing that could be completed using only finger motion, that is, without the hand or handrest. A 40 mm radius circle tested moderate curvature and required motion of the entire hand. Arcs of 100 mm radius presented a low curvature task that traversed the entire workspace.

Subject performance using the Active Handrest was compared to three alternate support conditions: fixed hand support, fixed elbow support, and “no support” (Fig. 6). In all conditions, the virtual writing surface and the support were positioned at the same nominal desk height. For fixed hand support, the subject used the Active Handrest as shown in Fig. 5, but the device did not move. For the fixed elbow support, the force sensor and handrest pad were removed, leaving only the non-moving elbow rest. In the “no support” case, the elbow rest was slid out of the way and the subject was required to manipulate the Omni stylus without any arm support. In the “no support” condition the user was allowed to comfortably position his/her arm, without overreaching, at the same drawing height used in the other conditions. These three cases were compared to the Active Handrest using force control input with a velocity limit of 5 mm/s, which was selected as the best case from pilot testing.

Each test block used a single support condition and tested subjects on 4 circles of each size for a total of 12 circles. Each block required approximately 10 minutes to complete and the entire test, including rest breaks between blocks, took subjects approximately 45 minutes. All blocks, for all experiments, and all subjects, presented the same order of circles. This order was generated with radii randomly chosen from the three radii discussed above. By repeating this same circle order for every block, we control for any effects of test order; any such interactions would affect all test conditions equally. To control for the effects of learning and fatigue as best as possible given our small subject pool, a Latin Squares ordering scheme was used to change the order of the test blocks between subjects.

The experiment was completed by 16 volunteer subjects. The subjects were classified in two groups: those that had prior experience with the Active Handrest (including the authors and those involved in pilot testing) and those that had no experience with the Active Handrest. For the group having prior experience using the device, there were 6 males and 2 females, ranging in age from 21 to 37 years. All but one were right hand dominant and 2 were authors involved in the development of the experiment. The left hand dominant participant used his non-dominant hand during the experiment. No significant trends in the results were observed due to this participant’s interaction with our device while using his non-dominant hand. For the group which had no prior experience using the device, there were 5 males and 3 females,

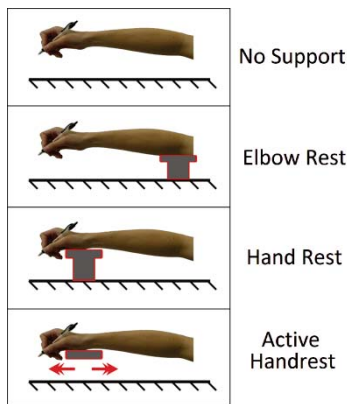


Figure 6. Examined experiment support conditions.

ranging in age from 23 to 41 years. Of these 8 subjects, all were right hand dominant.

All tests were completed under Institutional Review Board approved human subjects protocol.

## 5.2 Pilot Study Results and Discussion

Pilot tests using the circle tracing task were conducted to better tune the control of the Active Handrest before conducting a formal study. In our pilot study, we explored the effects of varying velocity limits, varying acceleration limits, and the percentage of force vs. position control to minimize error. Informal pilot tests included the authors as well as several other naïve subjects.

During each test, one of the following input methods was used to control the movement of the Active Handrest:

- force (isometric) input, using forces exerted on the handrest to command handrest motion;
- position (isotonic) input, using the position of the stylus to command handrest motion;
- blended input, using input both force and position input to control the handrest (50% of each).

By analyzing the results of the pilot studies, we were able to gain insight on how best to operate the Active Handrest. The first topic that we examined was the effect of stage motion velocity limits on tracing error. Velocity limits between 1 and 30 mm/s were examined. Drawing error was minimized at 5 mm/s for both the small circle and the large arc, and at 2.5 mm/s for the medium circle. However, because most subjects reported frustration with the sluggish motion of the Active Handrest below 5 mm/s, 5 mm/s was chosen as the velocity limit for the Active Handrest.

Additionally, we noted that error did not significantly change for velocity limits above 15 mm/s. We speculate that this trend was caused, in part, because users did not desire to perform the tracing tasks at speeds above 15 mm/s. Preliminary tracing completion time data supports this conclusion. We also decided to allow the stage to move at a maximum of 20 mm/s while repositioning the stage to get to the new drawing location.

Pilot study subjects noticed discontinuities in the Active Handrest’s motion, but only while the device was operating in force control mode. We determined that discontinuities were caused by feedback instabilities between the controller and the force sensor. The feedback instabilities were mitigated by implementing both a 1.6 Hz low-pass filter on the force sensor input and an acceleration limit on the stage’s motion. Low-pass filter corner frequencies between 0.85 and 16 Hz were examined. Acceleration limits between 0.5 and 5m/s<sup>2</sup> were examined. The acceleration limit was empirically set at 0.5 m/s<sup>2</sup>. This solution was found to eliminate the feedback instability in controlling the stage under force control, while causing no noticeable lag on stage velocity.

Additionally, the majority of the pilot test subject comments indicated a preference for force control when drawing circles and position control when repositioning the hand rest prior to and after drawing. The pilot test subjects remarked that the device felt more natural under force control and that the human-machine interface was more intuitive under force control than under position control. Although there was no significant improvement in accuracy, based on these comments we decided to operate the handrest under force control for our experiment.

## 5.3 Experiment Results and Discussion

The tracing task was difficult in part due to the non-collocated input from the stylus and the output reference on the screen. Such non-collocated tasks have been shown to present a challenge [13, 14]. Friction within the Omni device, resulting in stick-slip behavior of the stylus, also increased the difficulty of drawing

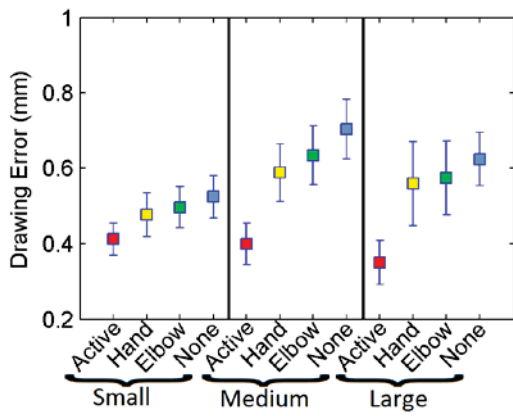


Figure 7. Pooled test results showing drawing error (left), grouped by circle size and support condition: Active Handrest, static handrest, elbow rest, and unsupported.

precise curves. As these factors influenced all test cases equally, they were not a concern in our analysis.

The experimental data were analyzed to extract information regarding drawing accuracy and drawing time. During the experiment, drawing data were collected at 100 Hz, producing a large volume of data for each circle. The drawing error was computed for each point as the distance from the drawn point to the target circle. The median drawing error was computed for each circle as a measure of performance. Mean error was not used because incidental subject mistakes, such as an accidental button click when traversing between circles, skewed the mean error value. The drawing time was also measured for each circle as the time between the first click of the drawing button to and its release at the completion of the circle.

Performance metrics were pooled from all subjects and averaged to produce Fig. 7, which shows mean performance (the mean of the subject median values) and 95% confidence intervals for each circle size and for each support condition, where performance is measured as the median error as described above. While drawing the small circle, there was no significant difference in error between support conditions. We expected error to be approximately the same in each case while drawing the small circle because the subjects were able to keep their hand in the center of its dexterous workspace regardless of the support method used. However, while drawing both the medium circle and the large arc, the Active Handrest was shown to provide a significant reduction in the amount of drawing error when

compared to the other three support methods ( $p < 0.001$ ). There was no significant difference in drawing error between the two static support methods or the unsupported condition. The significant decrease in error for the Active Handrest condition illustrates the device's utility while performing dexterous tasks over an expanded task area. Another interesting trend indicated by the data is that median drawing error decreased in the Active Handrest case as task complexity increased. Median error increased with task complexity, as expected, for each of the other three support conditions. Considering the small circle task as the baseline condition, this trend again highlights the usefulness of the Active Handrest.

As can be implied from Fig. 7, the drawing task for each of the circles had different difficulties. The pooled data were averaged for each circle size and are plotted in Fig. 8 (left). The small circle was the easiest task (statistically significant, ( $\alpha = 0.05$ ),  $F(2,765) = 7.65$ ,  $p < 0.001$ ), and the medium circle appears to be the most difficult, although the difference between the medium and large circles was not statistically significant. To observe a simpler measure of the benefit of the Active Handrest over the other support methods, the pooled data were averaged between all circles sizes and are presented in Fig. 8 (middle) as both error in mm and error normalized to the performance of the Active Handrest. This more simplified depiction of our results shows that use of the Active Handrest leads to less drawing error regardless of the tracing task chosen.

Figure 8 (right) shows the performance of each support method as a percent improvement over the unsupported case. A statistical analysis, using Tukey's method ( $\alpha = 0.05$ ), showed that the performance of the Active Handrest is statistically different than the other support methods ( $F(3,764) = 22.21$ ,  $p < 0.001$ ). The performance differences between the other support methods were not statistically significant. The data show that use of the Active Handrest leads to a 36.6% reduction in drawing error over the unsupported condition. Use of the Active Handrest also provides a 26.0% reduction in drawing error over static hand support.

### 5.3.1 Analysis of User Experience

This experiment was conducted on two groups of subjects: novice subjects who had no prior experience with the Active Handrest and experienced subjects who had participated in pilot experiments. A comparison between these two groups showed differences in both error and drawing time. Figure 9 shows pooled results for error (left) and time (right). The difference in drawing error between the two groups is large, with experienced users averaging approximately 40% less error than novice users. This difference is statistically significant ( $t(766) = -13.65$ ,  $p < 0.0001$ ).

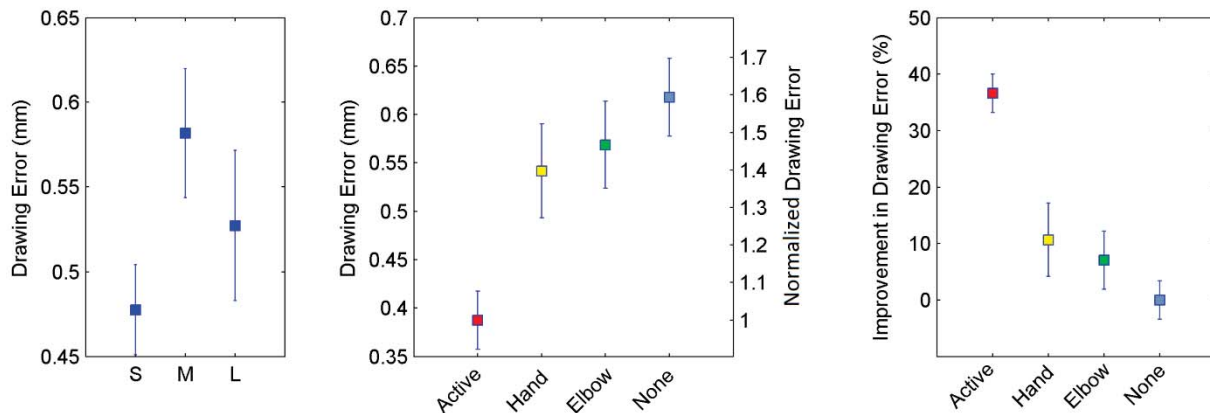


Figure 8. Combined test results showing drawing error grouped by circle size (left), support condition (middle), and drawing error shown as percentage improvement over the unsupported baseline condition (right).

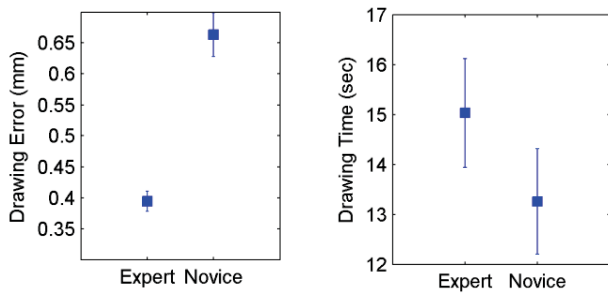


Figure 9. The effect of experience on drawing error (left) and drawing time (right).

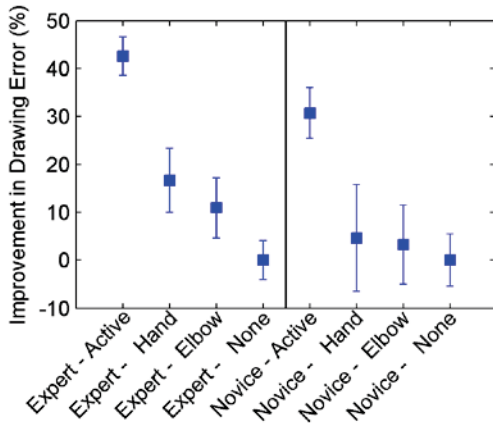


Figure 10. The effect of experience on relative performance. Experienced subjects derive more benefit from the Active Handrest.

The difference in time is also statistically significant ( $t(766) = 3.03, p = 0.003$ ), but relatively small with experienced users taking approximately 13% more time to complete the drawing tasks.

It is not surprising that users should perform better with experience when measured on an absolute scale, but the difference in relative improvement is more interesting. Relative improvement was calculated separately for novice and experienced subjects, with the “no support” data from each group serving as the baseline for that group. That is, experienced users were compared to experienced “no support” performance while novice users were compared to novice “no support” performance. The results are plotted in Fig. 10. Based on results reported in Fig. 10, the relative performance of the experienced subjects using the Active Handrest was significantly different than the novices ( $t(190) = 3.53, p = 0.0005$ ). While the absolute error data in Fig. 9 show that experienced subjects also performed better with practice, the relative data in Fig. 10 show that experienced users actually derived more benefit from the Active Handrest. This trend suggests that as users gain experience with the device, they learn to make better use of it. A similar analysis conducted on relative difference in drawing times did not show any interesting differences between experienced and novice subjects.

While these results are encouraging, it should be noted that the test groups were somewhat small (8 experienced users and 8 novice users). Therefore, the difference between the two groups could have been influenced by the characteristics of the specific subjects and may not be representative of population performance. Further testing will be required to conclusively determine the effects of experience with the Active Handrest.

### 5.3.2 Analysis of Drawing Time

Drawing times were also pooled from all subjects and are plotted in Fig. 11. It was found that drawing with the Active Handrest took longer than with any other support. This difference was statistically significant using Tukey's method ( $\alpha = 0.05$ ), ( $F(3,764) = 43.54, p < 0.001$ ). Although the Active Handrest was shown to require additional drawing completion time, previous work has shown that robot aided path following is typically slower than human path following alone [15].

It can also be assumed, and our data support, that slower drawing will result in less error. These drawing time results then raise the following question: does the Active Handrest actually provide any benefit other than forcing the user to draw slowly? To answer this question, we conducted an analysis of covariance to investigate the accuracy versus time relationship for all support types. This analysis reveals how accuracy varies with changing drawing time.

For small circles there is no statistically significant difference between the four support types ( $F(3,248) = 1.28, p = 0.282$ ). This lack of difference is in agreement with the data shown in Fig. 8; when drawing small circles there is little difference between the four different support conditions. For medium and large circles however, there are statistically significant differences. For both of these circle sizes the accuracy versus time relationship for both the Active Handrest and the “no support” condition are significantly different than the fixed hand and elbow supports. (For medium circles:  $F(3,248) = 13.99, p < 0.0001$ . For large circles:  $F(3,248) = 8.04, p < 0.0001$ .) For the Active Handrest and the no-support condition accuracy is relatively constant with respect to drawing time. In contrast, accuracy declines steeply when the user draws faster with the fixed hand and elbow supports.

This trend indicates that the Active Handrest does provide a real benefit; it allows a user to draw faster while maintaining uniformly high accuracy. In contrast, while using the fixed supports, accuracy is highly dependent on drawing speed. With the no-support condition accuracy was also relatively constant, but in this case it was uniformly low. That is, when drawing without support users performed poorly, regardless of the drawing speed.

An important implication of this analysis is as follows: had users been allowed to draw faster with the Active Handrest, they probably could have produced drawing times on par with the other support conditions while maintaining greater levels of accuracy. We do not consider this result conclusive, but it does begin to resolve the accuracy versus time question in favor of the Active Handrest. To fully understand how the Active Handrest affects drawing time and accuracy, additional experiments will be necessary.

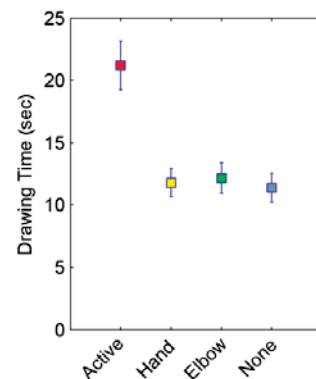


Figure 11. Test results showing circle drawing completion time.

## 6 FUTURE WORK

There exists great potential for further work on this subject. Initially, more analysis will be done on the data presented herein. Additional work will be conducted to optimize the controller. Additional experiments will be conducted to optimize the velocity and acceleration limits explored in our pilot studies. We will also directly correlate drawing error and drawing time to isolate the contributions attributed to using the Active Handrest.

It would also be interesting to compare the Active Handrest to additional methods of support, other devices, and other control methods, such as virtual fixtures. Virtual fixtures and/or cooperative control could be added to our environment to either assist the user in following an intended path or to avoid forbidden areas. Experiments could also be conducted on practical/real-world task performance such as pick and place tasks. Finally, the device could also be expanded to include a 3<sup>rd</sup> axis, thereby allowing tasks to be conducted in 3-DOF space instead of the current 2-DOF space.

## 7 CONCLUSIONS

We have presented and explored the efficacy of the Active Handrest, a novel device that assists a user in performing precision manipulation tasks over an extended work space, while reducing fatigue. We optimized the device by exploring isotonic (position), isometric (force), and blended control strategies while limiting the device's velocity and acceleration to improve device usability. We found that the Active Handrest enabled users to perform circle tracing tasks of varying difficulty while using a controller with the following properties:

- a hybrid admittance style controller that accepts both force and differential position inputs;
- closed-loop proportional control of stage velocity;
- isometric control with an acceleration limit of 0.5 m/s<sup>2</sup> and a velocity limit of 5 mm/s;
- force input low-pass filtered with corner frequency of 1.6 Hz.

We conducted an experiment with the Active Handrest using force input as its control strategy and compared its performance with various hand support conditions.

Our experimental results show the Active Handrest to be highly useful in assisting a user in performing precision manipulation tasks over a large workspace as follows:

- an improvement in task accuracy of 36.6% over the unsupported case (statistically significant:  $p < 0.001$ );
- an improvement in task accuracy of 26.0% over the best fixed support case – static handrest (statistically significant:  $p < 0.001$ );
- an increase in accuracy for users having prior experience with the device;
- decreased sensitivity on task error to work speed.

Through further exploration of the Active Handrest's utility, we believe that the device will be shown to be useful in assisting medical personal, artists, machinists, and others in performing precision tasks that require dexterous manipulation of tools over a large workspace.

## 8 ACKNOWLEDGEMENTS

This work was supported, in part, by the National Science Foundation under awards IIS-0746914 and DGE-0654414. We would also like to express our thanks to Dr. Jake Abbott for his input and advice on the device controller.

## REFERENCES

- [1] Bettini, A., et al., *Vision-assisted control for manipulation using virtual fixtures*. Robotics, IEEE Transactions on, 2004. **20**(6): p. 953-966.
- [2] Prada, R. and S. Payandeh, *A Study on Design and Analysis of Virtual Fixtures for Cutting in Training Environments*, in *Proceedings of the First Joint Eurohaptics Conference and Symposium on Haptic Interfaces for Virtual Environment and Teleoperator Systems*. 2005, IEEE Computer Society.
- [3] Ito, S. and Y. Yokokohji, *Maneuverability of master control devices considering the musculo-skeletal model of an operator*, in *Proceedings of the World Haptics 2009 - Third Joint EuroHaptics conference and Symposium on Haptic Interfaces for Virtual Environment and Teleoperator Systems*. 2009, IEEE Computer Society.
- [4] Taylor, R., et al., *A Steady-Hand Robotic System for Microsurgical Augmentation*. The International Journal of Robotics Research, 1999. **18**(12): p. 1201-1210.
- [5] Colgate, J.E., W. Wannasuphprasit, and M.A. Peshkin, *Cobots: Robots for collaboration with human operators*. Proc. ASME Dyn. Sys. Cont. Div., 1996. **DSC-58**: p. 433-440.
- [6] Rosenberg, L.B., *Virtual fixtures: Perceptual tools for telerobotic manipulation*. IEEE 1993 Virtual Reality Annual International Symposium, 1993: p. 76-82.
- [7] Abbott, J.J., P. Marayong, and A.M. Okamura, *Haptic Virtual Fixtures for Robot-Assisted Manipulation*. 12th International Symposium of Robotics Research (ISRR), 2005: p. 49-64.
- [8] Li, M. and A.M. Okamura, *Recognition of operator motions for real-time assistance using virtual fixtures*. in *Haptic Interfaces for Virtual Environment and Teleoperator Systems, 2003. HAPTICS 2003. Proceedings. 11th Symposium on*. 2003.
- [9] Zhai, S. and P. Milgram, *Quantifying coordination in multiple DOF movement and its application to evaluating 6 DOF input devices*, in *Proceedings of the SIGCHI conference on Human factors in computing systems*. 1998, ACM Press/Addison-Wesley Publishing Co.: Los Angeles, California, United States.
- [10] Zhai, S., *Investigation of Feel for 6DOF Inputs: Isometric and Elastic Rate Control for Manipulation in 3D Environments*. Human Factors and Ergonomics Society Annual Meeting Proceedings, 1993. **37**: p. 323-327.
- [11] Wu, M., J.J. Abbott, and A.M. Okamura, *Effects of velocity on human force control*. in *Eurohaptics Conference, 2005 and Symposium on Haptic Interfaces for Virtual Environment and Teleoperator Systems, 2005. World Haptics 2005. First Joint*. 2005.
- [12] Morris, D., Tan, H., Barbagli, F., Chang, T., and Salisbury, K., *Haptic Feedback Enhances Force Skill Learning*. in *Proceedings of IEEE World Haptics, 2007*.
- [13] Parsons, L., *Inability to reason about an object's orientation using an axis and angle of rotation*. Journal of Experimental Psychology: Human Perception and Performance, 1995. **21**(6): p. 1259-1277.
- [14] Ware, C. and R. Arsenault, *Frames of reference in virtual object rotation*, in *Proceedings of the 1st Symposium on Applied perception in graphics and visualization*. 2004, ACM: Los Angeles, California.
- [15] Kumar, R., P. Jensen, and R.H. Taylor. *Experiments with a steady hand robot in constrained compliant motion and path following*. in *Robot and Human Interaction, 1999. RO-MAN '99. 8th IEEE International Workshop on*. 1999.